Biochemical and Biophysical Research Communications 448 (2014) 274–280

Contents lists available at ScienceDirect

Biochemical and Biophysical Research Communications

journal homepage: www.elsevier.com/locate/ybbrc

Dystroglycan depletion inhibits the functions of differentiated HL-60 cells

Alma Delia Martínez-Zárate [a], Ivette Martínez-Vieyra [a], Lea Alonso-Rangel [a], Bulmaro Cisneros [b], Steve J. Winder [c], Doris Cerecedo [a,*]

[a] Laboratorio de Hematobiología, Escuela Nacional de Medicina y Homeopatía (ENMH), Instituto Politécnico Nacional (IPN), Mexico City, Mexico
[b] Departamento de Genética y Biología Molecular, Centro de Investigación y de Estudios Avanzados del IPN (Cinvestav-IPN), Mexico City, Mexico
[c] Department of Biomedical Science, University of Sheffield, Sheffield, UK

ARTICLE INFO

Article history:
Received 15 April 2014
Available online 30 April 2014

Keywords:
Dystroglycan
HL-60 cells
Differentiation
Phagocytosis
Respiratory burst activity
Migration

ABSTRACT

Dystroglycan has recently been characterized in blood tissue cells, as part of the dystrophin glycoprotein complex but to date nothing is known of its role in the differentiation process of neutrophils. We have investigated the role of dystroglycan in the human promyelocytic leukemic cell line HL-60 differentiated to neutrophils. Depletion of dystroglycan by RNAi resulted in altered morphology and reduced properties of differentiated HL-60 cells, including chemotaxis, respiratory burst, phagocytic activities and expression of markers of differentiation. These findings strongly implicate dystroglycan as a key membrane adhesion protein involved in the differentiation process in HL-60 cells.

1. Introduction

Haematopoiesis is the process leading to the sustained production of blood cells by hematopoietic stem cells (HSCs), giving rise to all hematopoietic lineage cells. Granulopoiesis describes a part of the haematopoiesis process in which a large number of granulocytes are formed by HSCs that can replicate and differentiate into multilineage cells (neutrophils, eosinophils, basophils) [1,2]. Haematopoiesis involves the coordination of several signal transduction pathways, which are induced by extracellular stimuli through cell–cell and cell–extracellular matrix (ECM) interactions [2]. Interactions with the ECM binding partners represent the critical steps by which cells initiate cytoplasmic signaling essential for the regulation of their growth, differentiation, attachment and migration, and are important factors in the development and progression of many types of cancer [3]. Dystroglycan (Dg) is an adhesion molecule responsible for crucial interactions between ECM and the cytoplasmic compartment [4]. It is formed by two subunits, α-Dg (extracellular) and β-Dg (transmembrane), that bind respectively to laminin in the matrix and to one of several cytolinker proteins such as dystrophin with the cytoskeleton [5]. As an integral part of the dystrophin glycoprotein complex (DGC) of skeletal muscle [6], dystroglycan is essential for signaling events mediated through this complex that may have a role as a mechanochemical, force-transducing system or shock-absorber [7] and indirectly mediating other signaling pathways associated with the DGC [8].

The human promyelocytic leukemia (HL-60) cell line can be induced to differentiate toward cells sharing several functional features of mature neutrophils [9] such as cell migration. Differentiated HL-60 cells (dHL-60) thus represent a valuable model system to study chemotaxis, and the contribution of the cytoskeleton in cell polarity [10].

We described previously the presence of DGC components in platelets, and demonstrated its central participation in the remodeling of cytoskeleton during the adhesion process; also our study showed the existence of DGC in resting and fMLP-treated human neutrophils. The interaction of the dystroglycan complex with the actin cytoskeleton is indicative of its dynamic participation in the chemotaxis process [11].

Therefore in this study, we chose the differentiated HL-60 cells as a model for human neutrophils to study the role of Dg in mature myeloid cells functions. We demonstrate here that Dg is intricately and essentially implicated in the differentiation process in neutrophils and so is therefore of considerable functional importance.

* Corresponding author. Address: Laboratorio de Hematobiología, Escuela Nacional de Medicina y Homeopatía, I.P.N., Guillermo Massieu Helguera No. 239, Col. La Escalera Ticomán, 07320 México, D.F., Mexico. Fax: +52 (55) 5729 6300x55532.
E-mail address: dcereced@prodigy.net.mx (D. Cerecedo).

http://dx.doi.org/10.1016/j.bbrc.2014.04.110
0006-291X/

2. Materials and methods

2.1. HL-60 cell culture and differentiation

HL-60 cells were cultured in RPMI-1640 medium supplemented with 10% fetal bovine serum, 400 mM L-glutamine, 50 μM gentamicin, 25 mM HEPES, 2 g/L sodium bicarbonate, 1 mM sodium pyruvate in a humid atmosphere of 5% CO_2 at 37 °C. For differentiation into a neutrophilic phenotype, HL-60 cells (dHL-60) were differentiated with 1.3% (v/v) DMSO for 7 days [12]. Cell viability was assessed by exclusion of 0.2% trypan blue and was routinely >90% before and after differentiation. For functionality assays dHL-60 cells were differentiated for 5 days with DMSO (Sigma–Aldrich) 1 μM. HL-60 cultures for some assays were cultured in presence of a furin inhibitor (decanoyl-RVKR-CMK) 200 μM for 2 days or during differentiation for 4 days.

2.2. Immunofluorescence staining

Antibodies used: α-dystroglycan clone VIA4-1 monoclonal antibody Cat. No. 05-298 was purchased from Millipore (Billerica, MA, USA), β-dystroglycan Cat. No. sc-30405 monoclonal antibody Cat. No. sc-21012, α-tubulin mAb Cat. No. sc-5286, were purchased from Santa Cruz Biotechnology, Inc. (Santa Cruz, CA, USA) and β-dystroglycan PY892 Cat. No. 617102 was purchased from Biolegend, (San Diego, CA, USA).

HL-60 cells were adhered with poly-D-lysine-coated coverslips and after 60 min were permeabilized and fixed with a mixture of 2% p-formaldehyde, 0.04% NP40 in the cytoskeleton stabilizing solution PHEM and triton 0.2%. HL-60 cells were first incubated with the specific primary antibodies diluted in PBS 0.1% bovine serum albumin to α-Dg and β-Dg diluted in PBS 0.5% bovine serum albumin for incubated for 24 h. Cells were washed with PBS solution and incubated for 1 h with secondary anti-goat, anti-mouse conjugated to Alexa-Fluor-488 (Molecular Probes, Eugene, OR, USA), cells were washed with PBS and incubated with phalloidin (Sigma Chemical Co.) to label the actin filaments for 30 min. For counterstaining, nuclei were dyed for 30 min with 4′,6-diami-dino-2-phenylindole (Sigma Chemical Co.), washed, and mounted. Slides were observed using a Leica confocal instrument model TCS-SP5 Mo, and images were taken at 63× zoom 3× at 1024 × 1024 pixels with an HCX PL APO 63×/1.40-0.60 DIL CS oil immersion. Optical sections [z] were captured at 0.18 mm. Immunofluorescence quantification was performed using ImageJ (NIH, Bethesda, USA). Filopodia size and number were detected using the software FiloDetect from images taken from fluorescence microscopy [13].

2.3. Western blotting analysis

HL-60 cells were resuspended and lysed with a 2× lysis buffer (0.5% NP-40, 2 mM Na_3VO_4, PSMF) containing a protease inhibitor cocktail. Homogenates were sonicated 3 times for 15 s. The protein concentrations were determined by the BCA method. The protein extract was mixed with loading buffer (Tris–HCl sodium dodecyl sulfate, β-mercaptoethanol, glycerol, bromophenol blue) and boiled for 5 min. Whole cell lysates were separated by 10% SDS–polyacrylamide gel electrophoresis (PAGE) and electrotransferred onto nitrocellulose membranes, using a semidry system (Thermo Fisher Scientific, Inc., Waltham, MA, USA). The protein bands were visualized with Ponceau. Membranes were washed with TBST-1× for 30 min and were blocked with 15% non-fat dried milk in TBST for 1 h. This was followed by incubation with appropriate primary antibodies overnight at 4 °C. The membrane was then washed and incubated with horseradish peroxidase conjugated anti-goat or mouse secondary antibodies (1:6000) in TBS/T for 60 min. After washing with TBS/T 3 times, enhanced chemiluminescence (ECL) assays were performed to visualize bands on X-ray films.

2.4. Plasmids and transfection

shRNA constructs targeting dystroglycan or control shRNA were generated using the RNAi- Ready pSiren-RetroQ system (Clontech Laboratories) have been described previously [14]. HL-60 cells (2×10^6/ml) were transfected with 2 μg DNA mixed with 2 μg pEGFP-N1 to mark the shRNA transfected cell population (Clon-Tech, Mountain View, CA, USA) on the Nucleofector II machine (Amaxa), according to the manufacturer's recommendation (Lonza Walkerrsville Inc. Walkersville, MD). Twenty-four hours after transfected cells were selected. For functional assays, selected cells were differentiated for 3 days.

2.5. Migration assay

dHL-60 KD Dg cell migration was evaluated using a 12-well Transwell chamber (Corning, Costar Corp). dHL-60 KD Dg cells were added to the upper chambers and allowed to migrate for 120 min at 37 °C in 5% CO_2 towards the lower chamber containing 10^{-7} fMLP. Migrated cells from lower chamber were centrifuged at 1200 rpm for 5 min, collected at the bottom of the lower chambers and quantified, the result was expressed as a percentage of cells added to the top of the plate.

2.6. Quantitative real-time PCR

Total RNA was extracted from HL-60 cells using Trizol Reagent RNeasy Mini Kit according to the manufacturer's instruction. 100 ng of total RNA was subjected to real-time PCR performed in triplicate using KAPA SYBR FAST (one step qRT-PCR kit) in a final volume of 10 μl. Reactions without a template or without the reverse transcriptase were used as negative controls. Amplification conditions consisted of an initial hot start at 42 °C for 5 min and 95 °C followed by amplification of 40 cycles (95 °C for 30 s, 60 °C for 1 min, and 72 °C for 30 s). PCR products were analyzed by the ΔΔCt method that compares the amount of target gene to an endogenous control (GAPDH), followed by normalization to a control sample to obtain relative levels of transcription.

2.7. Analysis of cell-surface antigens by immunofluorescence flow cytometry

Cells at 1×10^5/ml (100 μl) were incubated with monoclonal antibody for 30 min at 4 °C, washed twice with phosphate-buffered saline, and suspended for 30 min at 4 °C in 100 μl of Alexa 488-conjugated goat anti-rabbit IgG (Molecular probes Kallestad Laboratories, Inc., Austin, TX) previously diluted in phosphate-buffered saline. Then, cells were washed three times and subjected to immunofluorescence flow cytometer in a FACScan (Becton Dickinson San Jose, CA, USA). Fluorescence data were collected in log scale. Results were shown as percentages of positive cells for each antigen.

2.8. NBT reduction

Respiratory burst activity was measured by NBT (nitroblue tetrazolium) reduction as described previously [15]. Cells were stimulated with 50 ng/ml phorbol myristate acetate (PMA) for 15 min at 37 °C in the presence of 0.1% (w/v) NBT followed by centrifugation, washing (70% methanol), and addition of 2 M KOH to lyse the cells, and DMSO to dissolve the formazan blue pellet. NBT

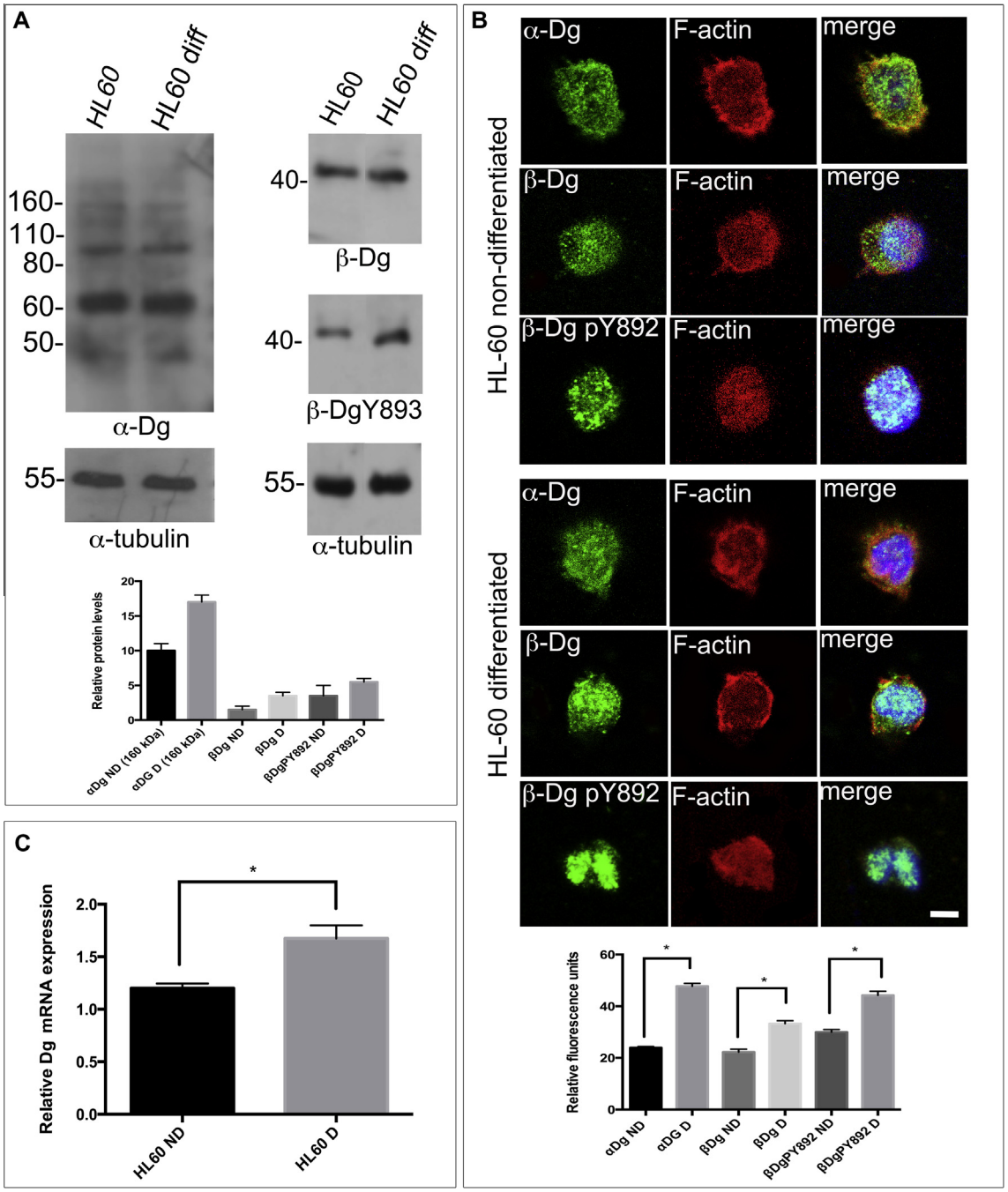

Fig. 1. Pattern expression and subcellular distribution of dystroglycans in HL-60 cells. (Panel A) Total lysates of HL-60 cells were analyzed by Western blot utilizing antibodies against C-terminal of α-Dg (160 kDa), β-Dg and βDgpY892. Quantitative analysis using tubulin as loading control is shown. Values shown are mean ± SEM from three independent experiments ($n = 3$), respectively. $^{*}P < 0.005$. (Panel B) HL-60 cells settled on glass cover slips were processed for double immunofluorescence using anti-dystroglycan antibodies (green), and counterstained with phalloidin (red) for visualization of the F-actin network and analyzed by confocal microscopy. Bar = 5 μm. Values shown are mean ± SEM from three independent experiments ($n = 3$), respectively. $^{*}P < 0.05$. (Panel C) (B) Messenger RNA expression of dystroglycan was examined by quantitative reverse transcription PCR in control and differentiated HL-60 cells. Values shown are mean ± SEM from three independent experiments ($n = 3$), respectively. $^{*}P < 0.05$. (For interpretation of the references to colour in this figure legend, the reader is referred to the web version of this article.)

reduction was quantified by the difference in the absorbencies at 620 and 450 nm.

2.9. Phagocytosis assays

Differentiated HL-60 cells were allowed to interact at 37 °C with phalloidin–TRITC-labeled *Candida glabrata*, at a yeast/cell ratio of 10:1. After a synchronized presentation, the samples were incubated at 37 °C for 30 min. Analysis was performed by flow cytometry in a FACScan (Becton Dickinson San Jose, CA, USA).

2.10. Statistical analysis

Statistical analysis was carried out with GraphPad Prism for Windows ver5 software (GraphPad Software, Inc., La Jolla, CA, USA). One-way Analysis of variance (ANOVA) with a multiple com-

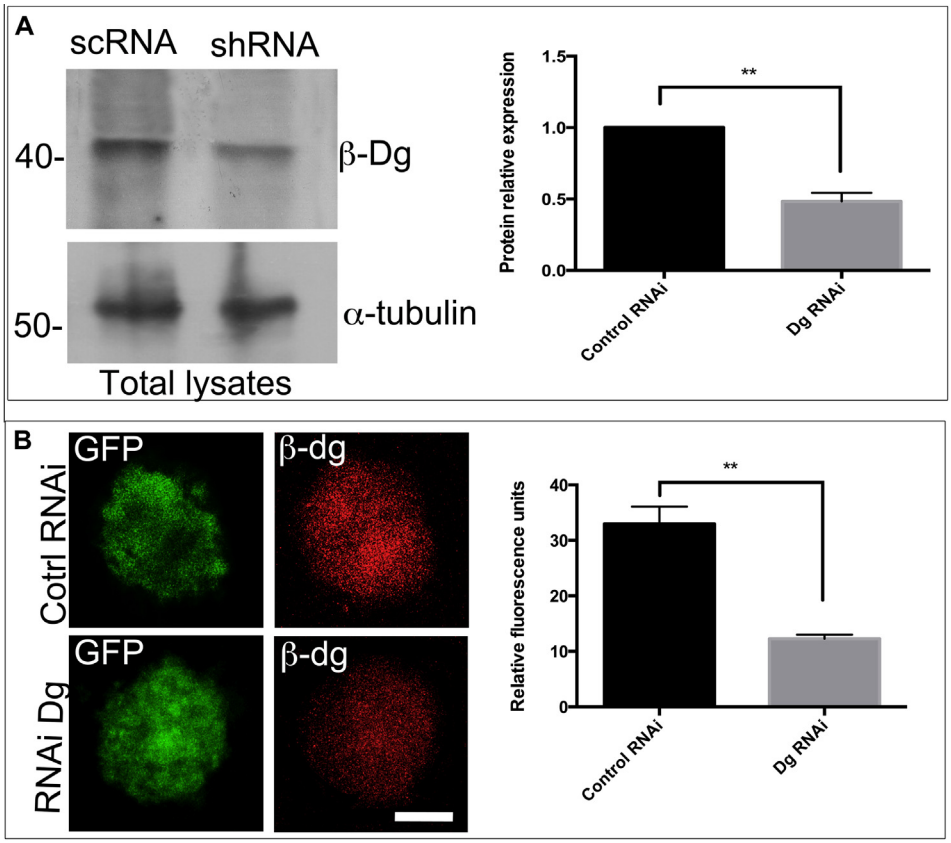

Fig. 2. RNAi mediated depletion of β-Dystroglycan in HL-60 cells. (Panel A) Total HL-60 cells extracts expressing either control RNAi or Dg RNAi were processed for Western-blot, utilizing an antibody against β-dystroglycan, corresponding bands were observed at 42 kDa. Densitometry analysis demonstrated β-Dg knockdown (50%) in cells transfected with a Dg iRNA as compared with cells transfected with a control iRNA. Values shown are mean ± SEM from three independent experiments ($n = 3$), respectively. $^{**}P < 0.001$. (Panel B) HL-60 cells extracts expressing either control RNAi or Dg RNAi were immunolabeled for β-dystroglycan and analyzed for confocal microscopy. Relative fluorescence units showed a significant knockdown of β-Dg. Values shown are mean ± SEM from three independent experiments ($n = 3$), respectively. $^{*}P < 0.002$.

parison test (Tukey test) was utilized for data analysis. Statistical significance was defined as $p < 0.05$.

3. Results

3.1. Dystroglycan is present in HL-60 cells

To determine the expression of dystroglycan (Dg) in differentiated and non-differentiated HL-60 cells, we performed Western blot assays using antibodies directed to the C-terminal segments of α-Dg, β-Dg and βDgPY892. Full-length α-Dg was revealed with a light band of 160 kDa, HL-60 cells for these assays were cultured in presence of decanoyl-RVKR-CMK a furin inhibitor; bands corresponding to 85 kDa, 60 kDa and 40 kDa were also detected. β-Dg and β-Dg phosphorylated on tyrosine 892 (β-DgPY892) were revealed with the presence of 43 kDa bands in both samples, however, the band corresponding to HL-60 differentiated cells (dHL-60) was clearly stronger than that of non-differentiated cells (ndHL-60) (Fig. 1, Panel A). Relative protein levels showed a statistical significance between, α-Dg, β-Dg and β-DgpY892 in dHL-60 and ndHL-60 cells (Fig. 1, Panel A).

To evaluate the subcellular distribution of Dg subunits, double immunofluorescence (IF) staining and confocal microscopy analysis on dHL-60 and ndHL-60 cells, were performed utilizing antibodies raised against α-Dg, β-Dg and βDgpY892 revealed with Alexa-Fluor-488 secondary antibody. Actin filaments were identified with Tetramethyl rhodamine iso-thiocyanate (TRITC)–phalloidin. In ndHL-60 cells, α-Dg subunit displayed a punctuated pattern distributed at the cytoplasm and the plasma membrane where it co-localized with actin filaments. This distribution was very similar to the distribution observed in differentiated cells. In both dHL-60 and ndHL-60 cells, β-Dg was observed with a discrete patched pattern at the cytoplasm, but in differentiated cells the label was stronger and was observed mainly located in the nuclei. Apparently most of the β-Dg corresponded to its phosphorylated form, which was also increased and mainly located in the nuclei (Fig. 1, Panel B). The relative fluorescence intensities showed values statistically significant (Fig. 1, Panel B).

To corroborate the increased level expression of dystroglycan subunits in non-differentiated and differentiated states observed by IF and Wb assays, we analyzed messenger RNA (mRNA) expression of dHL-60 and ndHL-60 cells by quantitative reverse transcription PCR (RT-qPCR). Fig. 1, Panel C, shows that mRNA expression of dystroglycans was significantly higher in dHL-60 cells compared to ndHL-60 cells ($p < 0.05$).

3.2. Effect of silencing Dg on dHL-60

As we had determined that there was an increase of Dg in dHL-60 cells, we attempted to ascertain whether β-dystroglycan is involved in the physiology of promyelocytic leukemia cells. In order to test this we analyzed how β-dystroglycan depletion influences the differentiation process of HL-60 cells by employing a small interfering RNA (RNAi) to target dystroglycan (Dg RNAi). The RNAi was co-expressed with GFP to identify unequivocally individual RNAi-treated cells. As negative control, RNAi that is predicted not to block the translation of any specific gene was utilized (control RNAi). Effectiveness of RNAi treatment in reducing

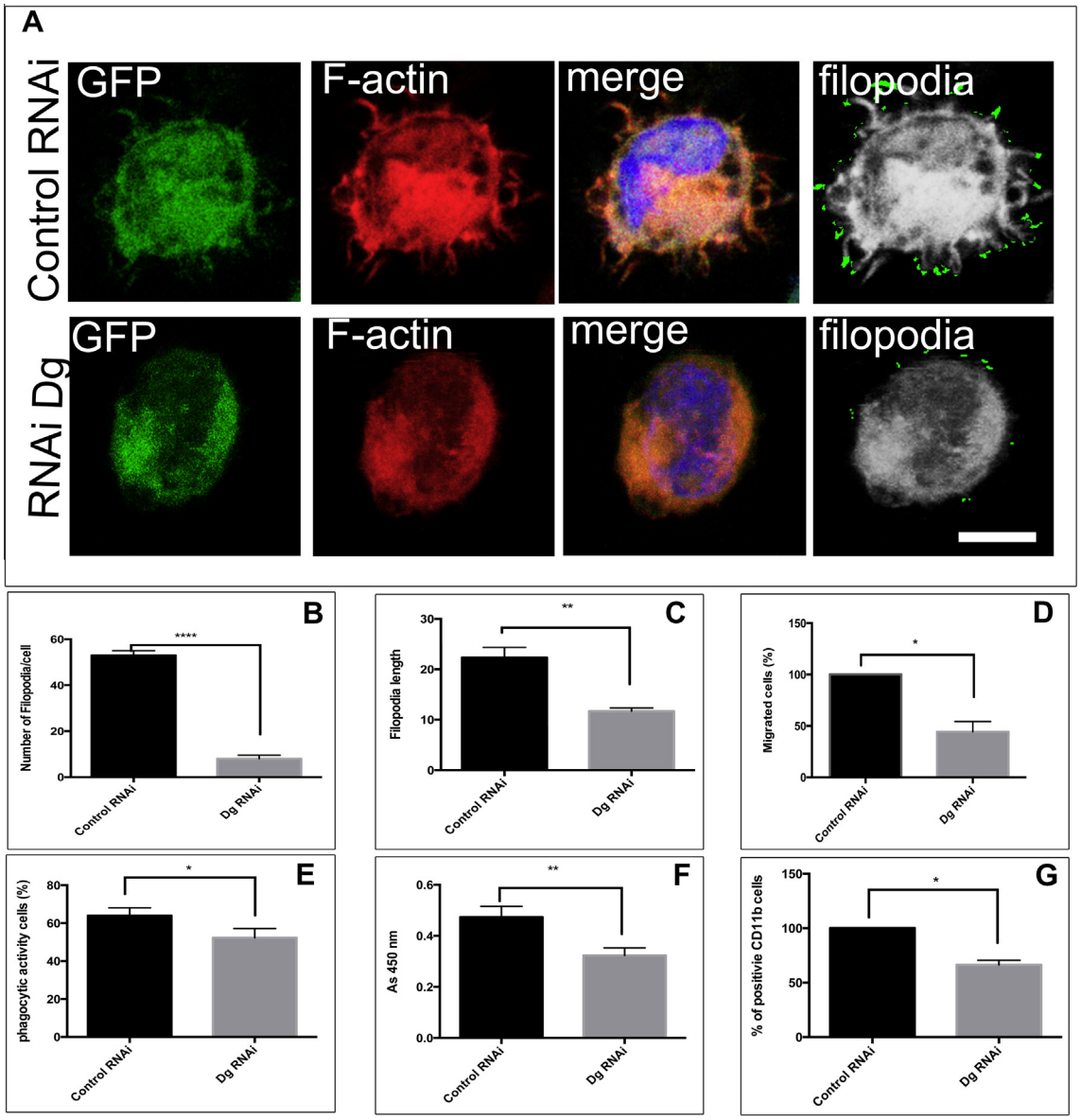

Fig. 3. β-Dystroglycan-deficient HL-60 cells fail to differentiate. (Panel A) HL-60 cells transfected with control and interference vector were analyzed by confocal microscopy to evaluate morphological changes in response to knockdown of dystroglycan. (Panel B) The number of filopodia was quantified by the FiloDetect software in 20 HL-60 RNAi-transfected cells that showed a low number of filopodia in relation to 20 control cells. Values shown are mean ± SEM from three independent experiments ($n = 3$), respectively. $^{****}P < 0.001$. (Panel C) The length of filopodia was quantified by the FiloDetect software in 20 HL-60 RNAi-transfected cells that showed shorter filopodia in relation to 20 control cells. Values shown are mean ± SEM from three independent experiments ($n = 3$), respectively. $^{**}P < 0.007$. (Panel D) The efficiency of migration was measured with a Transwell chamber and Dg-depleted HL-60 cells were less motile than control cells. Values shown are mean ± SEM from three independent experiments ($n = 3$), respectively. $^{*}P < 0.05$. (Panel E) Phagocytic ability is lost in Dg RNAi treated HL-60 cells compared to control HL-60 cells was evaluated by the internalization of *Candida glabrata* labeled with phalloidin–TRITC. Error bars show ±SEM, based on a total of three experiments; $^{*}p < 0.05$. (Panel F) The reduction of nitroblue tetrazolium (NBT) was measured and quantified by the absorbance at 450 nm of dissolved extracts from control RNAi- or Dg RNAi-treated HL-60 cells. Values shown are mean ± SEM from three independent experiments ($n = 3$), respectively. $^{**}P < 0.07$. (Panel G) CD11b levels were determined by flow cytometry. Relative CD11b levels obtained in control RNAi were set at 100%. Results are the mean ± SEM, based on a total of three experiments; $^{*}p < 0.05$.

β-dystroglycan expression in these cells was evaluated by Wb and IF assays. Global immunolabeling of β-dystroglycan was reduced by more than 50% in GFP-expressing cells that co-express Dg-specific RNAi, compared with control RNAi-treated cells (Fig. 2A). These levels of knock down are in keeping with studies in other cell lines using the same targeting sequences [11]. Intensity of the β-dystroglycan immunoreactive band (~43 kDa) was decreased by ~51% in cell lysates of HL-60 cells transiently transfected with vector expressing Dg RNAi but not in those expressing the control RNAi (Fig. 2 Panel A). DMSO–granulocyte-differentiated HL-60 cells exhibit similarities and differences with normal blood neutrophils [16,17]. In parallel with normal neutrophils, DMSO-differentiated HL-60 cells exhibit nuclear lobulation, nitroblue tetrazolium reduction by superoxide anions, enhanced expression of the cell surface antigen CD11b, and phagocytic capability.

To ascertain whether β-dystroglycan deficiency affects HL-60 function observed in dHL-60, control and β-dystroglycan-depleted cells were processed for double immunostaining to detect the presence of morphological changes following differentiation (Fig. 3, Panel A). The presence of filopodia was visualized in green with Filopodia_Code software (Fig. 3, Panel A, right side). β-dystroglycan-depleted differentiated cells exhibited a significant

diminution in the number of filopodia formed (mean 8 per cell) compared to control differentiated cells that protruded a mean of 53 per cell (Fig. 3, Panel B), while filopodia length was from 22 μm to 14 μm respectively (Fig. 3, Panel C).

To test the functional significance of the changes in number and length of filopodia we performed migration assays in Transwell chamber. Silencing of Dg expression significantly reduced the migration of dHL-60 cells compared to cells treated with RNA control. Dg RNAi reduced migration of dHL-60 cells to fMLP to 44.3% in relation to the RNA control (Fig. 3 Panel D). Similar results have been found in adherent cell types depleted for dystroglycan when analyzed for cell migration [11,21]. To assess the ability of cells to generate Superoxide anion, which is directly related to the differentiation process, we analyzed the ability of cells to reduce soluble NBT to blueblack insoluble formazan. The intensity of the absorbance registered for Dg RNAi in dHL-60 cells corresponded to a mean value of 0.324, significantly lower than in the HL-60 control cells, which exhibited a mean value of 0.474 (Fig. 3 Panel D). The phagocytic activity was present in 52.3% of Dg down-regulated dHL-60 cells compared to 63.9% of Dg control in dHL-60 cells (Fig. 3, Panel E). To further confirm if Dg expression affects the differentiation process in HL-60 cells we monitored the expression of CD11b, a well-established surface marker for differentiation. β-dystroglycan-depleted dHL-60 cells showed a diminution in the expression of CD11b compared to control dHL-60 cells, the mean values diminished to 63% (Fig. 3 Panel G).

4. Discussion

The human myeloid leukemia cell line (HL-60) has been widely investigated as a model for inducible cell differentiation and is capable of chemically induced cessation of cell division; all-trans-retinoic acid (ATRA) and dimethyl sulfoxide (DMSO) stimulate granulocytic differentiation [16,18]. In the present study we demonstrated that dystroglycans actively participate in the differentiation process.

We characterized the subcellular distribution and pattern of expression of α- and β-dystroglycan in HL-60 cells. Full length α-Dg of 160 kDa was visualized only after cells were cultured in the presence of decanoyl-RVKR-CMK, an inhibitor of proprotein convertase; it is feasible that this α-Dg cleavage may confer new functional roles as has been observed for PC12 [19]. Bands corresponding to 160 kDa, 85 kDa, 60 kDa and 40 kDa were identified, with the 60 kDa band being the most abundant. The expression levels of α-Dg (160 kDa), β-Dg (42 kDa) and β-DgpY892 (42 kDa) were increased in differentiated cells compared to non-differentiated cells as confirmed by qRT-PCR which correlated with an increase in mRNA for dystroglycan in differentiated cells (Fig. 1, Panel B,b).

DMSO treatment of HL-60 cells leads to a physiologically relevant differentiation process resulting in the cessation of the cell cycle, the appearance of differentiated granulocyte-like cells and a change in protein abundance [20]. It is likely that the classes and relative quantities of proteins present at the cell surface or other compartments at certain cellular stages are critical to regulate cellular functions. The plasma membrane versus the nucleus for example [21]. The differential expression of α- and β-dystroglycan were also evident by immunofluorescence microscopy, interestingly β-Dg and particularly β-DgpY892 were mainly located at the nuclei of differentiated HL-60 neutrophil cells; these findings strongly suggest their key participation in transcription processes that increases protein synthesis as a common feature during differentiation.

Both dHL-60 and nd-HL-60 cells reveal locomotor behavior. However, the induced cells migrate faster (comparable rate to normal neutrophils) and exhibit chemotactic responsiveness, which are not detectable in ndHL-60 cells [22,23]. Low levels of β-dystroglycan in dHL-60 cells are accompanied by the maintenance of a circular shape and altered filopodia extrusion as shown in Fig. 3. Similar phenotypes have also been described for oligodendrocytes [24]; in addition, alteration in filopodia number and length also affect concomitant cell motility. Dystroglycan has been proposed to be important for the maturation of adhesions into fibrillar adhesions and therefore in long-term adhesion and migration cells [25]. Circular shape of dystroglycan-depleted cells might be a consequence of increased ectopic and depolarized Cdc42 activation owing to mislocalization of a dystroglycan-Dbl complex, which leads to a loss of Cdc42 driven polarity [26]. HL-60 chemically induced differentiation leads to an increase in total cell actin (including both G- and F-actin), with parallel increases in actin-binding proteins (i.e., myosin and gelsolin) [27,28]. However, dHL-60 cells with a reduced level of dystroglycan have fewer actin-rich protrusions reducing motility and phagocytic capabilities. These changes are likely to be a direct consequence of the reduction in dystroglycan having an effect on actin cytoskeletal dynamics, not only through its ability to bind directly and indirectly to actin, but also through its ability to modulate the actin regulatory machinery through RhoGDI [8,26,29].

During differentiation, various characteristics of the HL-60 cell phenotype change, as the appearance of neutrophil cell surface antigens such as CD11b [30], as well as the ability to mount a plasma membrane oxidative burst in the vicinity of forming phagosomes [30]. According to our results, both the presence of azurophic granules as well as the percentage of a surface receptor (CD11b) were diminished compared to control cells, this leads us to suggest that that dystroglycan is a key protein for the maturation of HL-60 cells.

Our results have clinical implications as, in leukemic cells qualitative or quantitative changes in the adhesive properties may confer a proliferative advantage [31] affecting release of blast cells from the bone marrow microenvironment, thus, facilitating local proliferation or migration across the vessel wall into the circulation and subsequent development of extramedullary disease [32]. Changes in the expression level of dystroglycans in myeloid cells from leukemic patients may therefore serve as prognostic or diagnostic indicators in the clinic. This possibility is currently under investigation.

Acknowledgments

This work was supported by CONACYT-México, grant no. 161781. We thank the Unidad de Microscopía Confocal (Centro de Investigación y Estudios Avanzados del IPN) for technical assistance.

References

[1] I. Mavroudi, H.A. Papadaki, The role of CD40/CD40 ligand interactions in bone marrow granulopoiesis, ScientificWorldJournal 11 (2011) 2011–2019.
[2] C. Mazzon, A. Anselmo, J. Cibella, C. Soldani, A. Destro, N. Kim, M. Roncalli, S.J. Burden, M.L. Dustin, A. Sarukhan, A. Viola, The critical role of agrin in the hematopoietic stem cell niche, Blood 118 (2011) 2733–2742.
[3] A. Sgambato, M.A. Di Salvatore, B. De Paola, A. Rettino, B. Faraglia, A. Boninsegna, C. Graziani, A. Camerini, G. Proietti, A. Cittadini, Analysis of dystroglycan regulation and functions in mouse mammary epithelial cells and implications for mammary tumorigenesis, J. Cell Physiol. 207 (2006) 520–529.
[4] O. Ibraghimov-Beskrovnaya, J.M. Ervasti, C.J. Leveille, C.A. Slaughter, S.W. Sernett, K.P. Campbell, Primary structure of dystrophin-associated glycoproteins linking dystrophin to the extracellular matrix, Nature 355 (1992) 696–702.
[5] R. Barresi, K.P. Campbell, Dystroglycan: from biosynthesis to pathogenesis of human disease, J. Cell Sci. 119 (2006) 199–207.
[6] J.M. Ervasti, K. Ohlendieck, S.D. Kahl, M.G. Gaver, K.P. Campbell, Deficiency of a glycoprotein component of the dystrophin complex in dystrophic muscle, Nature 345 (1990) 315–319.

[7] S.J. Winder, The membrane-cytoskeleton interface: the role of dystrophin and utrophin, J. Muscle Res. Cell Motil. 18 (1997) 617–629.
[8] C.J. Moore, S.J. Winder, Dystroglycan versatility in cell adhesion: a tale of multiple motifs, Cell Commun. Signal. 8 (2010) 3.
[9] A.M. Santos-Beneit, F. Mollinedo, Expression of genes involved in initiation, regulation, and execution of apoptosis in human neutrophils and during neutrophil differentiation of HL-60 cells, J. Leukoc. Biol. 67 (2000) 712–724.
[10] A. Millius, O.D. Weiner, Chemotaxis in neutrophil-like HL-60 cells, Methods Mol. Biol. 571 (2009) 167–177.
[11] D. Cerecedo, B. Cisneros, P. Gomez, I.J. Galvan, Distribution of dystrophin- and utrophin-associated protein complexes during activation of human neutrophils, Exp. Hematol. 38 (2010) 618–628. e613.
[12] S.J. Collins, F.W. Ruscetti, R.E. Gallagher, R.C. Gallo, Terminal differentiation of human promyelocytic leukemia cells induced by dimethyl sulfoxide and other polar compounds, Proc. Natl. Acad. Sci. U.S.A. 75 (1978) 2458–2462.
[13] S. Nilufar, A.A. Morrow, J.M. Lee, T.J. Perkins, FiloDetect: automatic detection of filopodia from fluorescence microscopy images, BMC Systems Biol. 7 (2013) 66.
[14] G.M.A. Mitchell, T. Jiang, F.C. Hamdy, S.S. Cross, C. Eaton, S.J. Winder, Dystroglycan function is a novel determinant of tumor growth and behavior in prostate cancer, Prostate. 73 (2013) 398–408.
[15] F. Mollinedo, Isolation of human neutrophil plasma membranes employing neutrophil cytoplasts and changes in the cell-surface proteins upon cell activation, Biochim. Biophys. Acta 861 (1986) 33–43.
[16] S.J. Collins, The HL-60 promyelocytic leukemia cell line: proliferation, differentiation, and cellular oncogene expression, Blood 70 (1987) 1233–1244.
[17] T.R. Breitman, Growth and differentiation of human myeloid leukemia cell line HL60, Methods Enzymol. 190 (1990) 118–130.
[18] A. Yen, M. Forbes, G. DeGala, J. Fishbaugh, Control of HL-60 cell differentiation lineage specificity, a late event occurring after precommitment, Cancer Res. 47 (1987) 129–134.
[19] F. Saito, Y. Saito-Arai, A. Nakamura, T. Shimizu, K. Matsumura, Processing and secretion of the N-terminal domain of alpha-dystroglycan in cell culture media, FEBS Lett. 582 (2008) 439–444.
[20] A. Hofmann, B. Gerrits, A. Schmidt, T. Bock, D. Bausch-Fluck, R. Aebersold, B. Wollscheid, Proteomic cell surface phenotyping of differentiating acute myeloid leukemia cells, Blood 116 (2010) e26–34.
[21] G. Mathew, A. Mitchell, J.M. Down, L.A. Jacobs, F.C. Hamdy, C. Eaton, D.J. Rosario, S.S. Cross, S.J. Winder, Nuclear targeting of dystroglycan promotes the expression of androgen regulated transcription factors in prostate cancer, Sci. Rep. 3 (2013) 2792.
[22] W.H. Meyer, T.H. Howard, Actin polymerization and its relationship to locomotion and chemokinetic response in maturing human promyelocytic leukemia cells, Blood 70 (1987) 363–367.
[23] M.W. Verghese, T.B. Kneisler, J.A. Boucheron, P2U agonists induce chemotaxis and actin polymerization in human neutrophils and differentiated HL60 cells, J. Biol. Chem. 271 (1996) 15597–15601.
[24] C. Eyermann, K. Czaplinski, H. Colognato, Dystroglycan promotes filopodial formation and process branching in differentiating oligodendroglia, J. Neurochem. 120 (2012) 928–947.
[25] O. Thompson, C.J. Moore, S.A. Hussain, I. Kleino, M. Peckham, E. Hohenester, K.R. Ayscough, K. Saksela, S.J. Winder, Modulation of cell spreading and cell-substrate adhesion dynamics by dystroglycan, J. Cell Sci. 123 (2010) 118–127.
[26] C.L. Batchelor, J.R. Higginson, Y.J. Chen, C. Vanni, A. Eva, S.J. Winder, Recruitment of Dbl by ezrin and dystroglycan drives membrane proximal Cdc42 activation and filopodia formation, Cell Cycle 6 (2007) 353–363.
[27] W.H. Meyer, T.H. Howard, Changes in actin content during induced myeloid maturation of human promyelocytes, Blood 62 (1983) 308–314.
[28] R.G. Watts, Role of gelsolin in the formation and organization of triton-soluble F-actin during myeloid differentiation of HL-60 cells, Blood 85 (1995) 2212–2221.
[29] Y.J. Chen, H.J. Spence, J.M. Cameron, T. Jess, J.L. Ilsley, S.J. Winder, Direct interaction of beta-dystroglycan with F-actin, Biochem. J. 375 (2003) 329–337.
[30] P. Nordenfelt, S. Bauer, P. Lonnbro, H. Tapper, Phagocytosis of Streptococcus pyogenes by all-trans retinoic acid-differentiated HL-60 cells: roles of azurophilic granules and NADPH oxidase, PLoS One 4 (2009) e7363.
[31] E. Paietta, Adhesion molecules in acute myeloid leukemia, Leuk. Res. 20 (1996) 795–798.
[32] J.D. Cavenagh, E.C. Gordon-Smith, M.Y. Gordon, The binding of acute myeloid leukemia blast cells to human endothelium, Leuk. Lymphoma 16 (1994) 19–29.